Cold-developed electron-beam-patterned ZEP 7000 for fabrication of 13 nm nickel zone plates

Julia Reinspach,[a] Magnus Lindblom, Olov von Hofsten, Michael Bertilson, Hans M. Hertz, and Anders Holmberg
Department of Applied Physics, Royal Institute of Technology/Albanova, SE-10691 Stockholm, Sweden

(Received 30 June 2009; accepted 24 August 2009; published 1 December 2009)

Cold development was applied to improve the resolution in a trilayer resist that is used for the fabrication of state-of-the-art soft x-ray microscopy zone plates. By decreasing the temperature of the hexyl acetate developer to −50 °C, 11 nm half-pitch gratings have been resolved in the electron-beam resist ZEP 7000. 12 nm half-pitch gratings have been successfully transferred, via the intermediate SiO_2 hardmask, into the bottom polyimide layer by CHF_3 and O_2 reactive ion etching. The trilayer resist, including optimized cold development, has finally been used in an electroplating-based process for the fabrication of nickel zone plates. Zone plates with down to 13 nm outermost zone width have been fabricated and 2.4% average groove diffraction efficiency has been measured for zone plates with 15 nm outermost zone width and a nickel height of 55 nm.
 [DOI: 10.1116/1.3237140]

I. INTRODUCTION

Soft x-ray microscopy is used for nanoscale imaging in a wide range of applications in biology,[1,2] environmental science,[3] and magnetic studies.[4,5] The optics used for high-resolution imaging are nanofabricated diffractive optics, i.e., zone plates.[6,7] These are circular gratings with radially increasing line density. Presently, the optical performance of zone plate lenses is limited by the nanofabrication techniques. The difficulty in fabrication resides in the requirement for high diffraction efficiency and high resolving power. In order to obtain high diffraction efficiency the optical material must be thick enough to phase shift or attenuate the incoming x-rays.[8] The choice of the x-ray optical material depends on the wavelength, and for soft x-rays, nickel, germanium, and gold are commonly used. The resolving power, on the other hand, is determined by the width of the outermost zone, dr_N, which should be small.[7] To simultaneously satisfy these demands the optical material has to be structured with both high spatial resolution and high aspect ratio (AR). Since the zone plate pattern is dense, with line-to-space ratio of 1:1, the patterning alone becomes difficult for high-resolution zone plates. With the use of electron-beam lithography (EBL), zone plates with zone widths down to about 20 nm have been fabricated repeatedly.[9–12] However, the limitations of dense electron-beam patterning have impeded resolution improvements beyond this point. In order to achieve smaller zone widths, efforts have been made to circumvent the problem of dense patterning. One such method is the double patterning lithography technique implemented by Chao *et al.*,[13] which enabled the fabrication of zone plates with $dr_N=15$ nm. Another scheme, introduced by Jefimovs *et al.*,[14] utilizes a technique similar to sidewall lithography to double the effective line density of the electron-beam-written pattern.

In the present article we implement cold development into a standard trilayer resist process to increase the resolution in EBL. This enables dense patterning in a single exposure and without resorting to more complicated process steps such as those mentioned above. Using this method we demonstrate the fabrication of nickel zone plates with outermost zone width down to 13 nm. To our knowledge, this is the highest reported resolution for soft x-ray zone plates fabricated by a single electron-beam exposure. We have used ZEP 7000 developed in hexyl acetate and investigated the effect of developer temperature. It was found that cold development increases resolution and pattern quality. This is in agreement with previous studies on cold development of Poly(methyl methacrylate) (PMMA)[15–17] and ZEP 520.[15,18]

II. FABRICATION PROCESS FOR NICKEL ZONE PLATES

The fabrication process for high-resolution nickel zone plates is outlined in Fig. 1 and is similar to our previously used trilayer-resist-based process.[19] EBL and reactive ion etching (RIE) are used to structure a mold into which the nickel is deposited by electroplating. We have applied a trilayer resist to fabricate the mold since it enables the pattern to be written in a thin resist while still allowing high ARs to be structured. A thin resist is important for high-resolution EBL since it prevents line tilt in the development step and reduces the effect of forward scattering, which is particularly important for low acceleration voltages. In this work two different hardmask materials were used, either Ti or SiO_2. Ti has the benefit of a higher etch resistance in O_2 plasmas but SiO_2 provided higher reproducibility in the pattern transfer from the resist. The increased reproducibility was particularly pronounced for linewidths below 15 nm and SiO_2 was therefore used in the evaluation of cold development. Zone plates were fabricated using both materials.

X-ray transmissive Si_3N_4 membranes with a thickness of 50 nm were used as substrates. The membranes were first

[a]Electronic mail: julia.reinspach@biox.kth.se

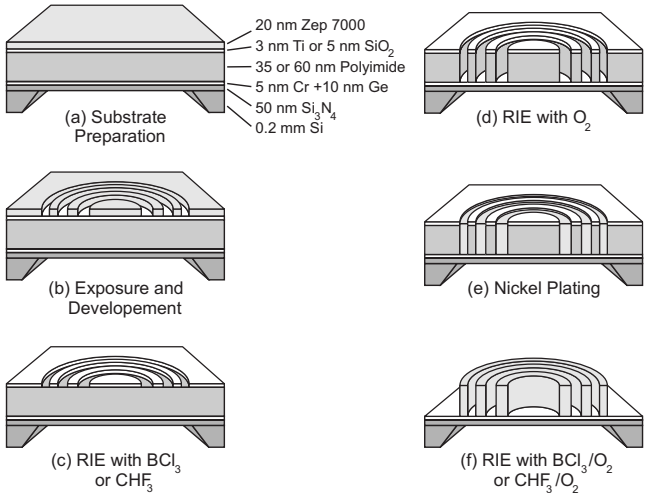

FIG. 1. Fabrication process for nickel zone plates. A trilayer resist is structured to a plating mold by e-beam lithography and two steps of reactive ion etching. The mold is filled with nickel by electrodeposition and subsequent removal of the mold completes the zone plate.

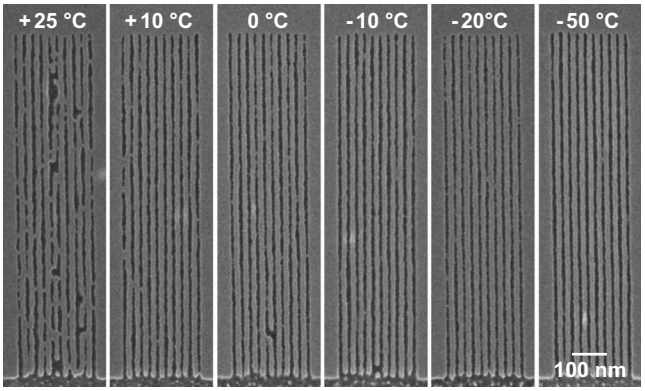

FIG. 2. SEM images of 12 nm half-pitch gratings etched 30 nm into a polyimide film. Development was performed at the indicated temperatures and it can be seen that the pattern quality improves with decreasing developer temperature.

coated with a plating base of 5 nm Cr and 10 nm Ge and then with a trilayer resist. The trilayer was composed of a 35 or 60 nm thick polyimide film (PI-2610, HD Microsystems), a hardmask consisting of either 3 nm Ti or 5 nm SiO_2 and a 20 nm thick electron-beam resist (ZEP 7000, Zeon Chemicals, L.P.). The plating base and the Ti hardmask were deposited by electron-beam evaporation (Edwards Auto 306, 10^{-6} Torr base pressure) at a rate of 0.2–0.4 Å/s. The SiO_2 was sputter deposited (AJA Orion, 10^{-8} Torr base pressure) at 3 mTorr pressure, 25 sccm (sccm denotes cubic centimeter per minute at STP) Ar flow, and a rate of 0.12 Å/s. The original polyimide was diluted in 1-methyl-2-pyrrolidon to give a thickness of 35 or 60 nm at a spin speed of 6000 rpm. Afterward, the baking was performed for 2 h at 350 °C. The original ZEP 7000 was diluted in diethylene glycol dimethyl ether to a thickness of 20 nm at 6000 rpm spin speed and then baked for 30 min at 170 °C.

The exposure was performed by EBL at 25 kV (Raith 150 system). The exposed resist pattern was developed in hexyl acetate, followed by a rinse step. Details concerning the exposure and development parameters are discussed in Sec. III. The developed pattern was then transferred to the hardmask by RIE. Samples with a Ti hardmask were etched with BCl_3 (Oxford Instruments, Plasmalab 80+) for a duration of 110 s using the following parameters: sample RF power of 80 W, pressure of 15 mTorr, and BCl_3 flow of 10 sccm. Samples with a SiO_2 hardmask were etched for 40 s with CHF_3 (Oxford Instruments, Plasmalab 100) using 25 W sample RF power, 10 mTorr pressure, and 10 sccm gas flow. Thereafter, the hardmask was used for the pattern transfer into the underlying polyimide mold by RIE with O_2 (Oxford Instruments, Plasmalab 80+). This etch was performed at 3 mTorr pressure, 50 W sample RF power, and 10 sccm O_2 flow. The polyimide etch rate was ~35 nm/min and the total etch time varied between 1 and 2 min depending on the thickness of the polyimide layer. The electrodeposition of nickel was carried out in a nickel sulfamate solution (Lectro-Nic10–03, Enthone OMI Inc.) at a temperature of 53 °C, a pH of 3.25, and a rate of 10–20 nm/min. After electroplating, the two RIE steps were repeated to remove the hardmask and the mold.

III. COLD DEVELOPMENT OF ZEP 7000

This section discusses cold development of ZEP 7000 in hexyl acetate. The effect on resolution was studied for developer temperatures from +25 to −50 °C, and contrast curves were measured to investigate the temperature dependence of contrast and sensitivity. For the resolution experiments, Si_3N_4 membranes were prepared with a trilayer resist as described in Sec. II and the electron-beam patterning was carried out at 25 kV and a beam current of 16 pA. To minimize the exposed line widths, gratings with half-pitch below 15 nm were exposed using the maximum possible line bias, i.e., by exposing single lines. The exposure dose varied from 80 $\mu C/cm^2$ for room temperature development up to 300 $\mu C/cm^2$ for development at −50 °C. The development time was 30 s, which ensured a sufficient clearing of narrow structures. After the development in hexyl acetate, the samples were rinsed for 3 s in isopropyl alcohol and 5 s in pentane and subsequently dried in a hot air flow.

The effect of cold development on resolution and pattern quality was evaluated with a scanning electron microscope (SEM) after pattern transfer via the hardmask and 30 nm etch into the polyimide mold. This ensures that the developed pattern quality is sufficient for a successful pattern transfer and therefore applicable for the zone plate fabrication process. Figure 2 shows gratings with 12 nm half-pitch, developed at different temperatures. An improvement in resolution and a reduction in pattern defects can be seen when decreasing the temperature from +25 to −50 °C. We do not observe an optimal cold development temperature, as was reported for PMMA at −15 °C.[16] For ZEP 7000, the pattern quality is significantly improved as the temperature is reduced from room temperature to below 0 °C. For the temperature range from 0 to −50 °C the change is less pronounced but we observe a continued enhancement of pattern quality down to

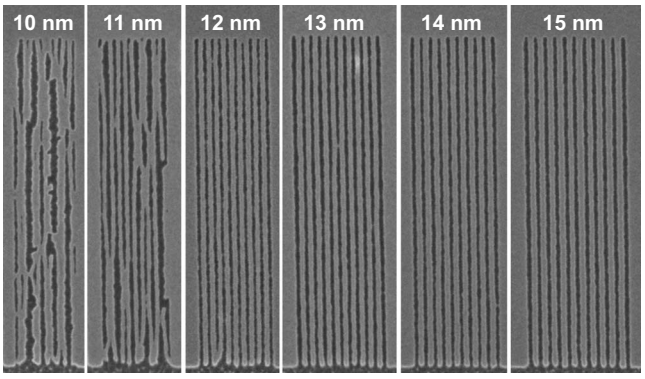

FIG. 3. Resolution limit for development at −50 °C is illustrated. The SEM images show 30 nm high polyimide-mold gratings with half-pitch from 10 to 15 nm. The 12–15 nm half-pitch gratings are clearly resolved and without pattern defects. In the 11 nm half-pitch grating the lines are resolved but some lines have collapsed. The 10 nm half-pitch grating is not resolved in this experiment.

−50 °C. Based on this experimental observation, we have chosen a developer temperature of −50 °C for the zone plate fabrication. At that temperature good pattern quality is ensured and the margin to the freezing point of the developer is wide enough to avoid problems with accidental freezing. Figure 3 shows gratings with 10 to 15 nm half-pitch, developed at −50 °C. Half-pitches down to 12 nm are clearly resolved and without pattern defects. The grating with 11 nm half-pitch is also resolved, but individual grating lines have tilted. The tilt probably occurred in the O_2 etch step. Alternatively, the ZEP 7000 could have tilted when dried after development due to a too high aspect ratio and surface tension forces.

Contrast curves were measured for developer temperatures ranging from +30 to −60 °C. For this experiment, a Si wafer was prepared with 160 nm thick ZEP and exposed at 25 kV. The exposed structures were then developed for 30 s and the residual resist thickness was determined by scanning profilometry (Tencor P15). The results are shown in Fig. 4. It

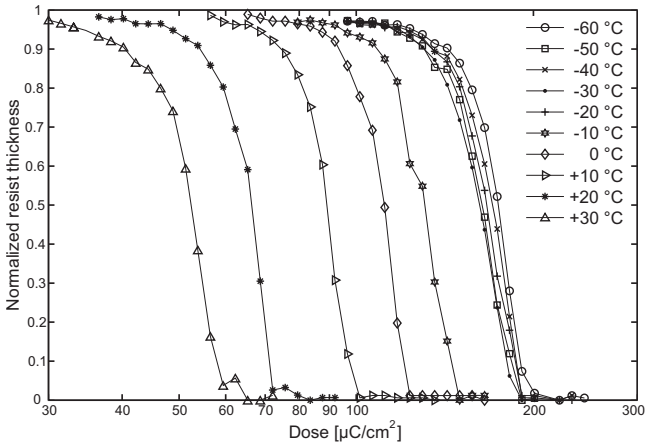

FIG. 4. Contrast curves for ZEP 7000 developed in hexyl acetate at different developer temperatures. The dose-to-clear saturates for temperatures below −20 °C. No change in contrast, i.e., no change in the slope of the linear falling part of the curve can be concluded.

can be seen that the sensitivity decreases when lowering temperature, reaching a constant value for temperatures below −20 °C. From our measured data, no change in contrast with temperature can be concluded, i.e., we cannot measure a change in slope of the linearly falling part of the curve. However, the contrast curves indicate that there is a difference in the transition region between undeveloped and partly developed resist, i.e., in the region left of the linearly falling part of the curves. This transition is more gradual for room temperature development. This suggests that the relative dose difference from totally undeveloped resist to fully developed resist is larger for room temperature development. For high-resolution dense patterns like gratings, where all resist between exposed lines is exposed to some extent, this could explain the observed resolution improvement for low development temperatures. The influence of development time on contrast and on sensitivity was also investigated by taking contrast curves at −50 °C for development times from 15 s up to 90 s. Within this parameter range, no significant change in contrast or sensitivity could be observed.

IV. FABRICATED ZONE PLATES

The resolution improvement due to cold development enabled the fabrication of nickel zone plates with outermost zone width dr_N down to 13 nm. Figure 5 shows details of three zone plates with dr_N of 15, 14, and 13 nm, which were fabricated using a development temperature of −50 °C. The displayed area is limited but the depicted pattern quality is representative for the full zone plate. In terms of pattern defects and line-to-space ratio, these high-resolution zone plates are comparable in quality with our 25 nm zone plates.[11]

The 15 nm zone plate had a diameter of 26 μm and a focal length of 157 μm at $\lambda = 2.48$ nm. The nickel thickness was measured with a scanning profilometer (Tencor P15) to be 55 nm on average. The zone plates with 14 and 13 nm outermost zone widths had diameters of 18 and 19 μm, respectively, and their focal lengths were 100 μm at $\lambda = 2.48$ nm. The average nickel thickness was 35 nm.

The 15 nm zone plate was characterized in terms of diffraction efficiency. This measurement was carried out at $\lambda = 2.88$ nm in a laboratory laser-plasma-based arrangement.[20] The first-order diffraction efficiency was measured to be $2.4 \pm 0.4\%$, which corresponds to ~50% of the maximum theoretical efficiency[8] at $\lambda = 2.88$ nm and a zone height of 55 nm. For comparison, zone plates with $dr_N = 25$ nm, which we fabricated earlier, were measured to have ~70% of their theoretical diffraction efficiency.[20] The deviation from the theoretical value is due to imperfections in the zone plates, such as line edge roughness and suboptimal line-to-space ratio. The zone plates with $dr_N < 15$ nm have so far not been measured due to constraints in the efficiency measurement arrangement.

V. SUMMARY AND OUTLOOK

We have introduced cold development of the EBL-exposed resist in our standard trilayer process for the fabri-

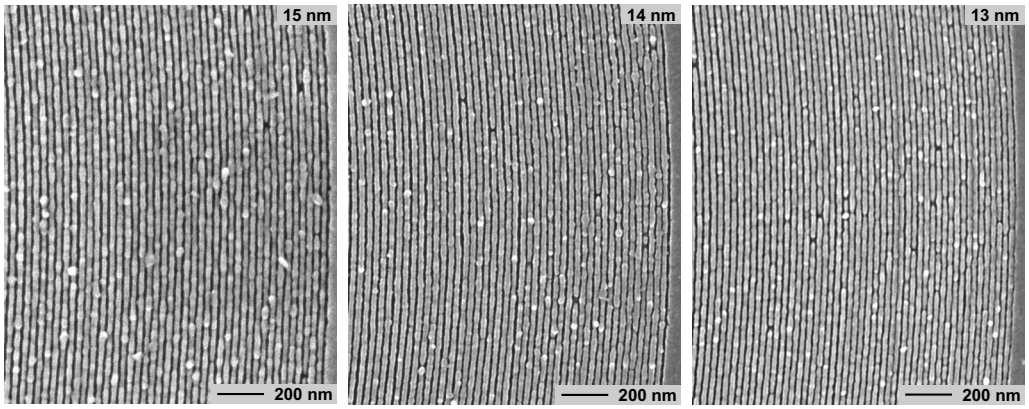

FIG. 5. Detailed view of the outermost part of nickel zone plates with 15, 14, and 13 nm outermost zone widths.

cation of nickel zone plates. This has enabled the fabrication of zone plates with down to 13 nm outermost zone width, which is to our knowledge the highest reported resolution for soft x-ray zone plates fabricated by a single electron-beam exposure. For the zone plates with 15 nm outermost zone width and 55 nm zone height, the average diffraction efficiency was determined to $2.4 \pm 0.4\%$ at $\lambda = 2.88$ nm.

In cold development experiments with ZEP 7000 developed in hexyl acetate, we have shown that the achievable resolution increases with reduced developer temperature. At a developer temperature of $-50\ ^\circ\mathrm{C}$, gratings with half-pitch down to 11 nm have been resolved in the resist and 12 nm half-pitch gratings have successfully been transferred into the bottom polyimide layer of the trilayer resist.

In the near future the zone plates will be implemented in soft x-ray microscopes for high-resolution imaging. To allow more accurate diffraction-efficiency measurements for zone plates with a small diameter and small dr_N, the experimental arrangement for this purpose will be redesigned and improved.

ACKNOWLEDGMENTS

The authors thank K. Jefimovs for sharing his experience with polyimide processing. They also gratefully acknowledge the financial support of the Swedish Science Research Council, the Swedish Foundation for Strategic Research, the Wallenberg Foundation, and the Göran Gustafsson Foundation.

[1] D. Y. Parkinson, G. McDermott, L. D. Etkin, M. A. Le Gros, and C. A. Larabell, J. Struct. Biol. **162**, 380 (2008).
[2] S. C. B. Myneni, J. T. Brown, G. A. Martinez, and W. Meyer-Ilse, Science **286**, 1335 (1999).
[3] J. Thieme, S. C. Gleber, P. Guttmann, J. Prietzel, I. Mcnulty, and J. Coates, Miner. Mag. **72**, 211 (2008).
[4] B. L. Mesler, P. Fischer, W. Chao, E. H. Anderson and D.-H. Kim, J. Vac. Sci. Technol. B **25**, 2598 (2007).
[5] P. Fischer, IEEE Trans. Magn. **44**, 1900 (2008).
[6] *X-ray Microscopy*, edited by S. Aoki, Y. Kagoshima, and Y. Suzuki (Institute of Pure and Applied Physics, Tokyo, Japan, 2006), Vol. 7.
[7] D. T. Attwood, *Soft X-Rays and Extreme Ultraviolet Radiation* (Cambridge University Press, Cambridge, 1999), pp. 337–394.
[8] J. Kirz, J. Opt. Soc. Am. **64**, 301 (1974).
[9] M. Peuker, Appl. Phys. Lett. **78**, 2208 (2001).
[10] S. J. Spector, C. J. Jacobsen, and D. M. Tennant, J. Vac. Sci. Technol. B **15**, 2872 (1997).
[11] A. Holmberg, M. Lindblom, S. Rehbein, and H. M. Hertz, in *Proceedings of the Eighth International Conference on X-ray Microscopy* (Institute of Pure and Applied Physics, Tokyo, Japan, 2006), p. 124.
[12] M. Lindblom, J. Reinspach, O. v. Hofsten, M. Bertilson, H. M. Hertz, and A. Holmberg, J. Vac. Sci. Technol. B **27**, L1 (2009).
[13] W. Chao, B. D. Harteneck, J. A. Liddle, E. H. Anderson, and D. T. Attwood, Nature (London) **435**, 1210 (2005).
[14] K. Jefimovs, J. Vila-Comamala, T. Pilvi, J. Raabe, M. Ritala, and C. David, Phys. Rev. Lett. **99**, 264801 (2007).
[15] L. E. Ocola and A. Stein, J. Vac. Sci. Technol. B **24**, 3061 (2006).
[16] B. Cord, J. Lutkenhaus, and K. K. Berggren, J. Vac. Sci. Technol. B **25**, 2013 (2007).
[17] W. C. Hu, K. Sarveswaran, M. Lieberman, and G. H. Bernstein, J. Vac. Sci. Technol. B **22**, 1711 (2004).
[18] H. Wang, G. M. Laws, S. Milicic, P. Boland, A. Handugan, M. Pratt, T. Eschrich, S. Myhajlenko, J. A. Allgair, and B. Bunday, J. Vac. Sci. Technol. B **25**, 102 (2007).
[19] A. Holmberg, S. Rehbein, and H. M. Hertz, Microelectron. Eng. **73–74**, 639 (2004).
[20] M. Bertilson, P. A. C. Takman, U. Vogt, A. Holmberg, and H. M. Hertz, Rev. Sci. Instrum. **78**, 026103 (2007).